ISSN 1674-1056
http://cpb.iphy.ac.cn
http://iopscience.iop.org/cpb
中国物理 B
Chinese Physics
中国物理 Chinese Physics B

Effect of Mo doping on phase change performance of Sb_2Te_3

Wan-Liang Liu(刘万良), Ying Chen(陈莹), Tao Li(李涛), Zhi-Tang Song(宋志棠), and Liang-Cai Wu(吴良才)
Citation: Chin. Phys. B, 2021, 30 (**8**): 086801. DOI: 10.1088/1674-1056/abe22d
Journal homepage: http://cpb.iphy.ac.cn; http://iopscience.iop.org/cpb

What follows is a list of articles you may be interested in

Scalable preparation of water-soluble ink of few-layered WSe_2 nanosheets for large-area electronics

Guoyu Xian(冼国裕), Jianshuo Zhang(张建烁), Li Liu(刘丽), Jun Zhou(周俊), Hongtao Liu(刘洪涛), Lihong Bao(鲍丽宏), Chengmin Shen(申承民), Yongfeng Li(李永峰), Zhihui Qin(秦志辉), Haitao Yang(杨海涛)
Chin. Phys. B, 2020, 29 (**6**): 066802. DOI: 10.1088/1674-1056/ab889e

PEALD-deposited crystalline GaN films on Si (100) substrates with sharp interfaces

San-Jie Liu(刘三姐), Ying-Feng He(何荧峰), Hui-Yun Wei(卫会云), Peng Qiu(仇鹏), Yi-Meng Song(宋祎萌), Yun-Lai An(安运来), Abdul Rehman(阿布度-拉赫曼), Ming-Zeng Peng(彭铭曾), Xin-He Zheng(郑新和)
Chin. Phys. B, 2019, 28 (**2**): 026801. DOI: 10.1088/1674-1056/28/2/026801

High quality $PdTe_2$ thin films grown by molecular beam epitaxy

En Li(李恩), Rui-Zi Zhang(张瑞梓), Hang Li(李航), Chen Liu(刘晨), Geng Li(李更), Jia-Ou Wang(王嘉鸥), Tian Qian(钱天), Hong Ding(丁洪), Yu-Yang Zhang(张余洋), Shi-Xuan Du(杜世萱), Xiao Lin(林晓), Hong-Jun Gao(高鸿钧)
Chin. Phys. B, 2018, 27 (**8**): 086804. DOI: 10.1088/1674-1056/27/8/086804

Formation of high-Sn content polycrystalline GeSn films by pulsed laser annealing on co-sputtered amorphous GeSn on Ge substrate

Lu Zhang(张璐), Hai-Yang Hong(洪海洋), Yi-Sen Wang(王一森), Cheng Li(李成), Guang-Yang Lin(林光杨), Song-Yan Chen(陈松岩), Wei Huang(黄巍), Jian-Yuan Wang(汪建元)
Chin. Phys. B, 2017, 26 (**11**): 116802. DOI: 10.1088/1674-1056/26/11/116802

Optoelectronic properties of SnO_2 thin films sprayed at different deposition times

Allag Abdelkrim, Saâd Rahmane, Ouahab Abdelouahab, Attouche Hafida, Kouidri Nabila
Chin. Phys. B, 2016, 25 (**4**): 046801. DOI: 10.1088/1674-1056/25/4/046801

Effect of Mo doping on phase change performance of Sb_2Te_3*

Wan-Liang Liu(刘万良)[1,2], Ying Chen(陈莹)[1,2], Tao Li(李涛)[1,2], Zhi-Tang Song(宋志棠)[1], and Liang-Cai Wu(吴良才)[3,4,†]

[1] *State Key Laboratory of Functional Materials for Informatics, Shanghai Institute of Micro-system and Information Technology, Chinese Academy of Sciences, Shanghai* 200050, *China*

[2] *University of Chinese Academy of Sciences, Beijing* 100049, *China*

[3] *College of Science, Donghua University, Shanghai* 201620, *China*

[4] *Member of Magnetic Confinement Fusion Research Center, Ministry of Education, China*

(Received 15 December 2020; revised manuscript received 28 January 2021; accepted manuscript online 2 February 2021)

Mo, as a dopant, is doped into SbTe to improve its thermal stability. It is shown in this paper that the Mo-doped Sb_2Te_3 ($Mo_{0.26}Sb_2Te_3$, MST) material possesses phase change memory (PCM) applications. MST has better thermal stability than Sb_2Te_3(ST) and will crystallize only when the annealing temperature is higher than 250 °C. With the good thermal stability, MST-based PCM cells have a fast crystallization time of 6 ns. Furthermore, endurance up to 4×10^5 cycles with a resistance ratio of more than one order of magnitude makes MST a promising candidate for PCM applications.

Keywords: phase-change memory, Sb_2Te_3, thin films, nanocomposites

PACS: 68.35.bd, 68.37.Yz, 68.60.Dv **DOI:** 10.1088/1674-1056/abe22d

1. Introduction

As one of the most potential alternatives for next-generation non-volatile memory (NVM),[1,2] phase change memory (PCM) has the advantages of fast programming speed, high scalability, and non-volatility.[3–5] By phase transition between amorphous state (high-resistance) and crystalline state (low-resistance), information is stored in PCM.[6] Owing to its fast switching speed between amorphous state and crystalline state, SbTe is one of the most widely studied phase change materials and has been applied to high speed phase change storage.[7–11] However, the poor thermal stability restricts the further application of SbTe. Therefore, some impurities, such as Si,[12] N,[13] and Al,[14] are doped into the pure SbTe system to improve its performance. But these doping impurities bring some adverse effects to PCM. For example, Si doping results in phase separation in $Si_2Sb_2Te_6$,[12] nitrogen atoms combine and escape from NSb_2Te_3,[13] and Al oxidation in $AlSb_3Te$ reduce their usefulness in practical applications of PCM.[14]

In our previous work, we have studied Mo-doped $Sb_{1.8}Te$,[15] whose speed and thermal stability are better than those of $Ge_2Sb_2Te_5$. However, the operation voltage is large (> 3.5 V). Here, we propose a Mo-doped Sb_2Te_3 ($Mo_{0.26}Sb_2Te_3$, MST) material. It is found that the MST based PCM device has an operation time of 6 ns, which is faster than the operation time of Mo-doped $Sb_{1.8}Te$ (10 ns). More importantly, the operation voltage of MST (2.5 V@20 ns) is much lower than that of Mo-doped $Sb_{1.8}Te$ (4.5 V@20 ns), indicating a much lower power consumption. Furthermore, MST can maintain its amorphous state at room temperature until the annealing temperature reaches higher than 250 °C. The resistance contrast between amorphous state and crystalline state is largely increased, offering a larger sensing margin for applications.

2. Experiments

The Sb_2Te_3 and Mo-doped Sb_2Te_3 (ST) samples were deposited on a SiO_2/Si(100) substrate by magnetron co-sputtering using Mo and Sb_2Te_3 targets at ambient temperature, where the background pressure and working pressure were set to be 2×10^{-4} Pa and 0.21 Pa, respectively. The concentration was evaluated by energy dispersion x-ray spectrometry (EDS; Oxford INCA Energy equipped in Hitachi S4700 scanning electron microscope). Sheet resistance as a function of temperature (R–T) was studied by Linkam LMP 95 hot stage. The XRD measurements in a 2θ range of 10°–60° were employed to characterize the structures of the films, which were annealed for 3 min under pure N_2 atmosphere at temperatures of 150 °C, 200 °C, and 250 °C, respectively. T-shaped test cells with 190-nm-diameter W electrodes have been fabricated using 0.13-μm CMOS technology. Then ∼ 100-nm MST film was deposited on the W electrodes, followed by depositing a 10-nm-thick TiN adhesion layer and 200-nm-thick Al on the top electrode. The electrical properties of MST-based PCM were measured by Keithley 2400C and Tektronix AWG5002B pulse generator. Besides, ∼ 15-nm-thick ST and

*Project supported by the National Key Research and Development Program of China (Grant Nos. 2017YFB0701703 and 2017YFA0206101), the National Natural Science Foundation of China (Grant No. 61874151), and the Science and Technology Council of Shanghai, China (Grant Nos. 19JC1416801 and 19JC1416802).

†Corresponding author. E-mail: lcwu@dhu.edu.cn

© 2021 Chinese Physical Society and IOP Publishing Ltd

MST films were deposited directly on supporting grids coated with carbon film and then annealed under pure N_2 atmosphere at 250 °C for 3 min to investigate their microstructure by using the transmission electron microscopy(TEM), high-resolution TEM (HRTEM), and selected area electron diffraction (SAED).

3. Results and discussion

We first measure the sheet resistance as a function of temperature (R–T) for each of ST and MST, and the results are shown in Fig. 1(a). The resistance of as-deposited undoped ST film is $\sim 3 \times 10^4$ Ω, and after having been Mo-doped, the resistance of as-deposited film increases by an order of magnitude, which can contribute to reducing the power consumption. But the increase in the resistance of crystalline state is not so significant, indicating a larger sensing margin for applications.

Figures 1(b) and 1(c) show the XRD patterns of ST and MST, which are annealed at different temperatures. Most of the diffraction peaks correspond to FCC and HEX phase of Sb_2Te_3, and no other diffraction peaks corresponding to Mo or Te are found. It can be found that diffraction peaks appear in the as-deposited ST film, while diffraction peaks appear in the MST film only when the annealing temperature is higher than 200 °C, reflecting the fact that the as-deposited state of ST is polycrystalline while the as-deposited state of MST is amorphous, and MST crystallize only when annealing temperature is higher than 200 °C, indicating a big boost in thermal stability by Mo doping. This also corresponds to the fact that as-deposited state of ST is composed of polycrystals. When annealing temperature is higher than 150 °C, the phase of ST turns from FCC to HEX, while FCC phase appears in MST only when annealing temperature is 200 °C and disappears when temperature is higher than 250 °C. The full width at half maximum of MST is much wider than that of ST at the same annealing temperature, which means that the grain size of MST is much smaller than that of ST when being annealed at the same temperature. The shrinking of the size of Mo-doped grain implies that the Mo atoms suppress the growth of crystal grains of ST.

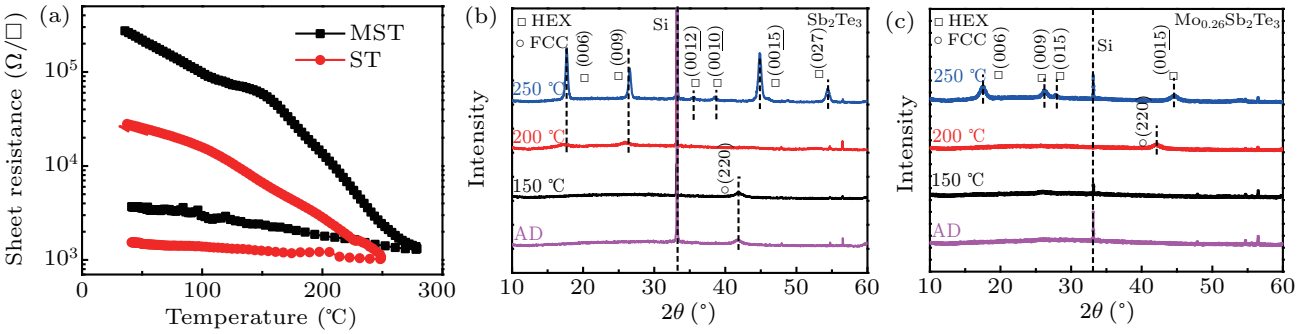


Fig. 1. (a) The R–T curves of ST film and MST film at heating rate of 20 °C/min, XRD patterns of (b) ST and (c) MST annealed at different temperatures.

In order to further obtain the information about the crystal structure of ST and MST, the TEM, HRTEM, and SAED are carried out for investigation. The final crystal structures of ST and MST films after annealing at 250 °C for 3 min are shown in Fig. 2. The comparison between Fig. 2(a) and Fig. 2(d) reveals that the grain size of ST is $\sim$ 100 nm, however, by Mo doping, the grain size of MST decreases to only several nanometers. As the grain size decreases, the surface-to-volume ratioincreases, increasing the electron scattering at grain boundaries, thus increasing the electrical resistivity.[16] By comparing our measured interplanar crystal spacing and the angle between them with their corresponding standard values, we can conclude that both ST and MST have the same crystal structure as HEX Sb_2Te_3, without other phase appearing, in correspondence with the results of XRD.

Figure 3(a) shows the T-shaped test cells with 190-nm-diameter W electrodes: the Al bottom electrode, SiO_2 isolation layer, and W heating electrode are prepared by using the 0.13-μm CMOS technology. Then $\sim$ 100-nm MST film is deposited on the W electrode, followed by by depositing a 10-nm-thick TiN adhesion layer and 200-nm-thick Al top electrode. Figure 3(b) shows that with the current increasing, the voltage increases gradually, but sharply drops when the voltage is 2.6 V and the current is 2 μA. This is because under this voltage, the device changes from amorphous to crystalline state, and the resistance decreases sharply, which reflects the sudden drop of voltage. After this threshold switch, with the gradual increase of current, the voltage also maintains a linear increase. This means that the resistance is maintained at a stable value. Figure 3(c) shows the curve of resistance changing with the pulse height under different pulse widths: the resistance changes from high to low and then to high with pulse voltage increasing, indicating that SET operation and RESET operation can be realized under these pulse widths. When the pulse width decreases from 100 ns to 6 ns, the SET and RESET voltages increase gradually. Because the energy is consumed certainly, when the pulse width decreases, the height of the pulse must be increased accordingly. It is worth mentioning that the SET operation and the RESET operation can be realized under 6-ns pulse width, which is about an order of mag-

nitude faster than that of $Ge_2Sb_2Te_5$ (GST) ($\sim$ 50 ns) and it is also faster than that of the Mo-doped $Sb_{1.8}Te$ (10 ns). The reset voltage in Fig. 3(c) is 2.5 V@20 ns and 3.2 V@6 ns, which is lower than that of the Mo-doped $Sb_{1.8}Te$ (4.5 V@20 ns). The result in Fig. 3(d) shows that $\sim 4 \times 10^5$ stable reversible switch between high resistance and low resistance can be realized with an operating voltage of 2.4 V and a pulse width of 50 ns for the SET operation, and an operating voltage of 4 V and a pulse width of 20 ns for the RESET operation. These results indicate that the MST is a promising candidate for high-speed phase change memory applications with good thermal stability.

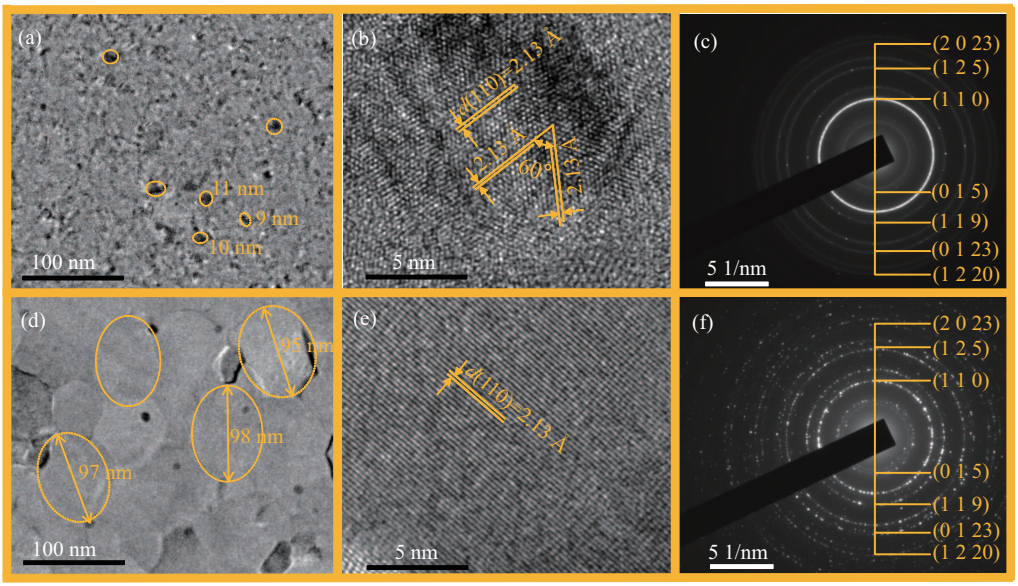


Fig. 2. (a) TEM image, (b) HRTEM image, and (c) SAED pattern of MST, (d) TEM image, (e) HRTEM image, and (f) SAED pattern of ST.

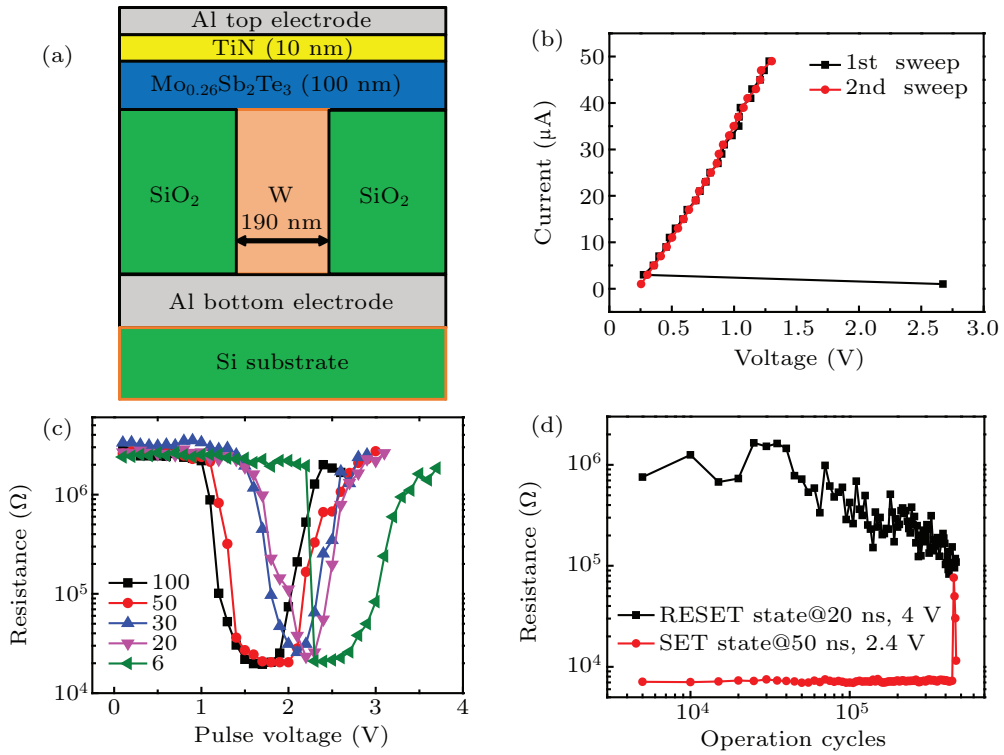


Fig. 3. (a) The cross-sectional structure of PCM cell, (b) *I*–*V* curves, (c) *R*–*V* characteristics, and (d) durability of cells based on MST.

4. Conclusions

In this study, Mo doping is a promising way of improving the thermal stability of ST. The MST can be maintained in amorphous state at room temperature, thus greatly improving the potential applications of ST. With Mo-doped, MST has smaller grain size and higher electrical resistivity without changing crystal structure. Moreover, a high speed PCM cell is made from MST and exhibits a 6-ns phase change, low opera-

tion voltage, and $\sim 4 \times 10^5$ successful cycles. These outstanding properties confirm that Mo dopant is an excellent method of improving the phase change performance of ST.

References

[1] Fujimori S, Yagi S, Yamazaki H and Funakoshi N 1988 *J. Appl. Phys.* **64** 1000

[2] Friedrich I, Weidenhof V, Njoroge W, Franz P and Wuttig M 2000 *J. Appl. Phys.* **87** 4130

[3] Wuttig, M 2005 *Nat. Mater.* **4** 265

[4] Wuttig M and Yamada N 2007 *Nat. Mater.* **6** 824

[5] Yin Y, Sone H and Hosaka S 2007 *J. Appl. Phys.* **102** 064503

[6] Zhou X L, Wu L C, Song Z T, Rao F, Liu B, Yao D N, Yin W J, Li J T, Feng S L and Chen B 2009 *Appl. Phys Express* **2** 091401

[7] Chen N K and Li X B 2019 *Chin. Phys. B* **28** 104202

[8] Liu B, Liu W L, Li Z, Li K Q, Wu L C, Zhou J, Song Z T and Sun Z M 2020 *ACS Appl. Mater. Interfaces* **12** 20672

[9] Chang C C, Kao K F, Tsai M J, Yew T R and Chin T S 2011 *J. Nanosci Nanotechnol.* **11** 12

[10] Peng C, Song Z T, Rao F, Wu L C, Zhu M, Song H J, Zhou X L, Yao D N, Yang P X and Chu J H 2011 *Appl. Phys. Lett.* **4** 99

[11] Sun Z M, Zhou J, Mao H K and Ahuja R 2012 *PNAS* **109** 5948

[12] Zhang B, Zhang W, Shen Z J, Chen Y J, Li J X, Zhang S B, Zhang Z, Wuttig M, Mazzarello R and Ma E 2016 *Appl. Phys. Lett.* **108** 191902

[13] Zhou X L, Kalikka J, Ji X L, Wu L C, Song Z T and Simpson R E 2016 *Adv. Mater.* **28** 3007

[14] Rao F, Ding K Y, Zhou Y X, Zheng Y H, Xia M J, Lv S L, Song Z T, Feng S L, Ronneberger I and Mazzarello R 2017 *Science* **358** 1423

[15] Liu W L, Wu L C, Li T, Song Z T, Shi J J, Zhang J and Feng S 2018 *Appl. Phys. Express* **11** 041401

[16] Meng Y, Behera J K, Wen S, Simpson R E, Shi J J, Wu L C, Song Z T, Wei J S and Wang Y 2018 *Adv. Opt. Mater.* **6** 1800360